Supporting Information

Exosome-based rare earth nanoparticles for targeted *in situ* and metastatic tumor imaging with chemo-assisted immunotherapy

Bi Lin,[a] *Yanxing Wang,*[a] *Kun Zhao,*[b] *Wei-Dong Lü,*[b,*] *Xin Hui,*[a] *Yaqun Ma,*[a] *and Ruichan Lv* [a,*]

[a] Engineering Research Center of Molecular and Neuro Imaging, Ministry of Education, School of Life Science and Technology, Xidian University, Xi'an, Shanxi 710071, China. Email: rclv@xidian.edu.cn

[b] Department of Thoracic Surgery, Tumor Hospital of Shaanxi Province, Affiliated to the Medical College of Xi'an Jiaotong University, Xi'an, Shaanxi 710061, China. Email: wdlu76@126.com

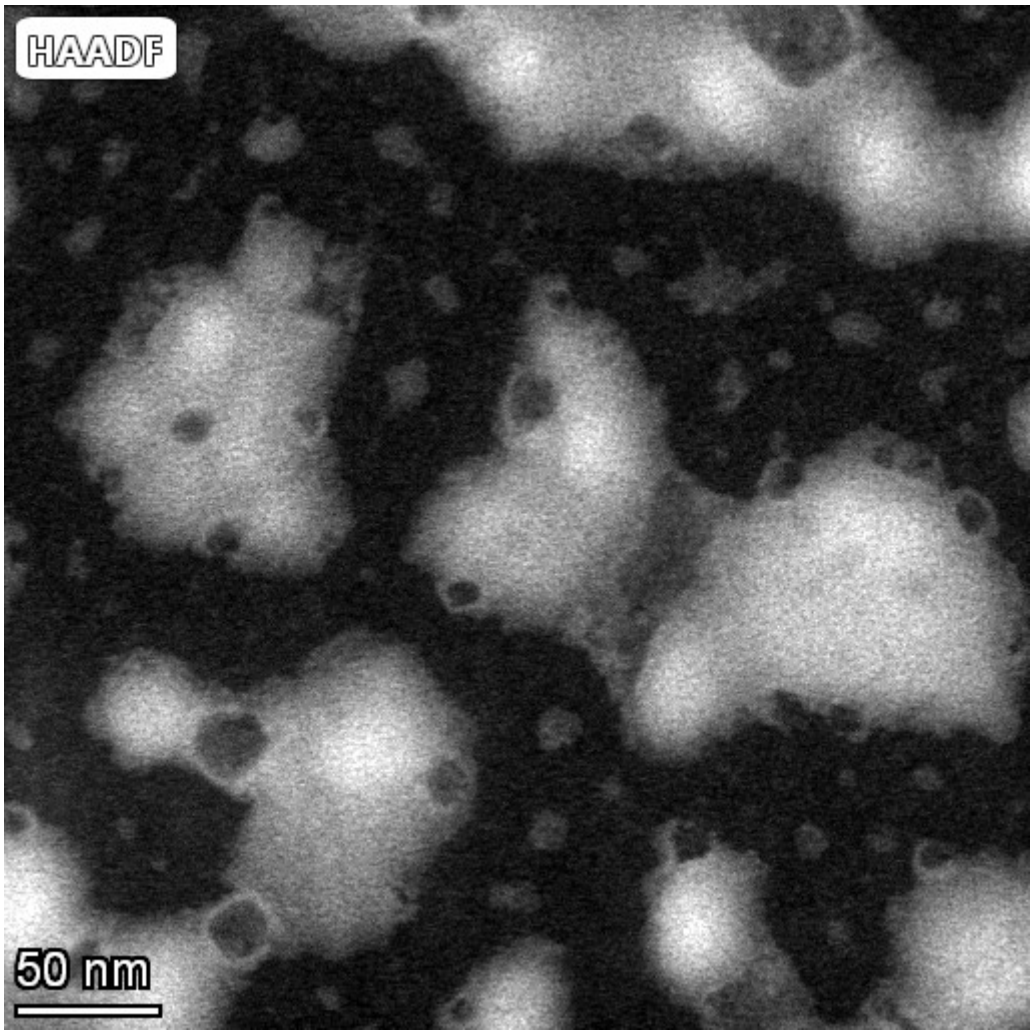

Figure S1. The element mapping overlay of the E-RENPs.

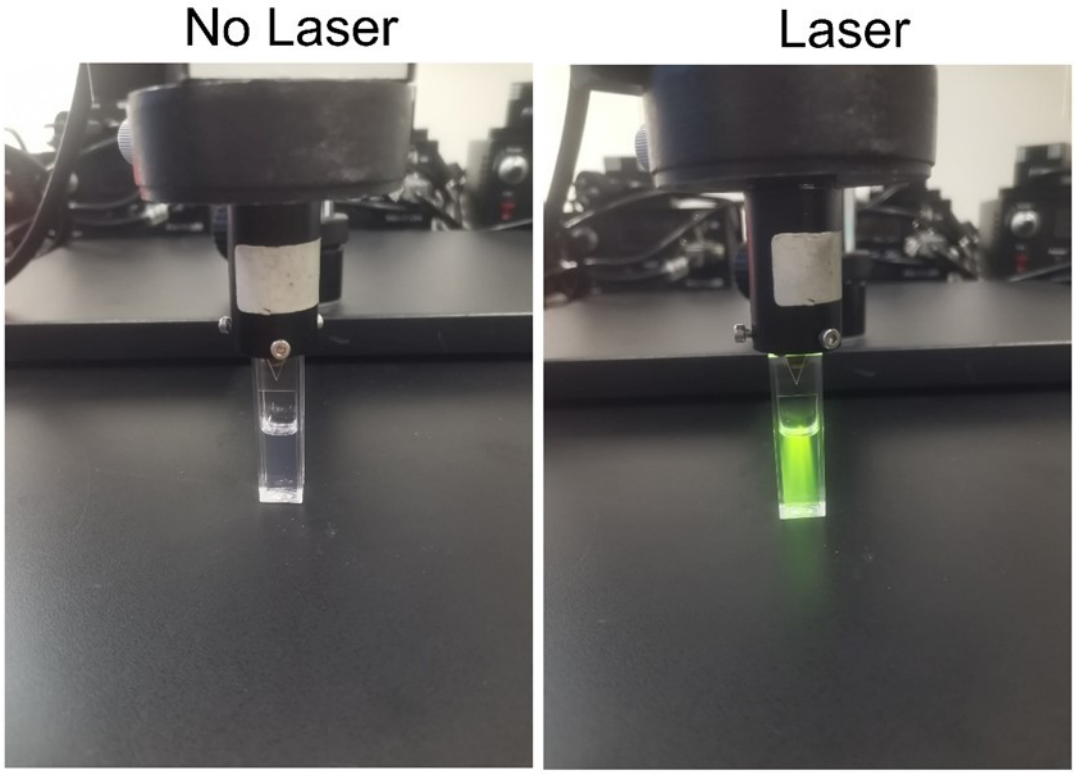

Figure S2. Under the irradiation of 980 nm laser, the UCL fluorescence imaging of RENPs..

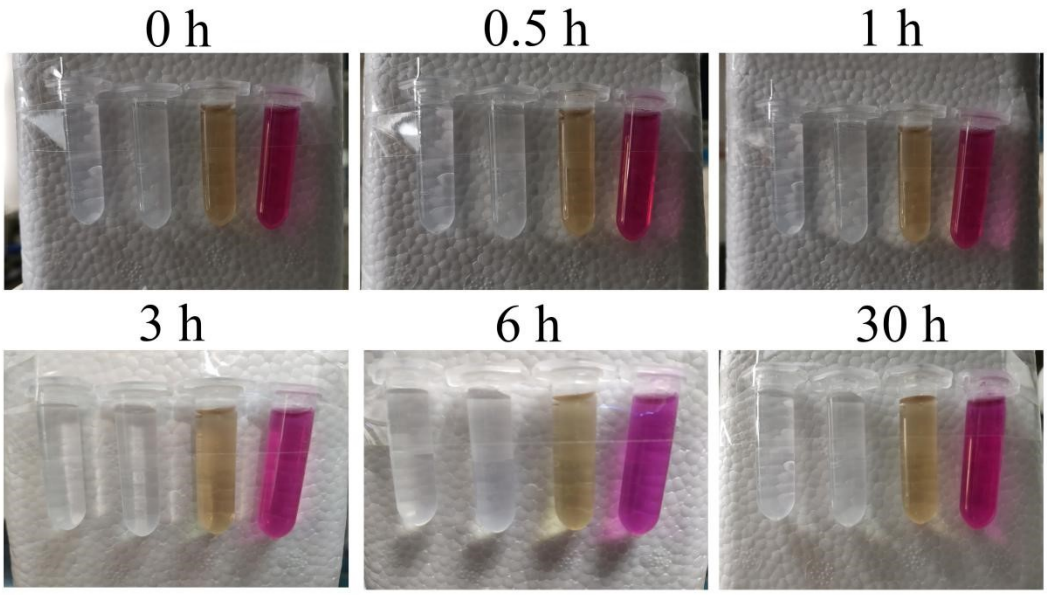

Figure S3. The biostability photographs of RENPs.

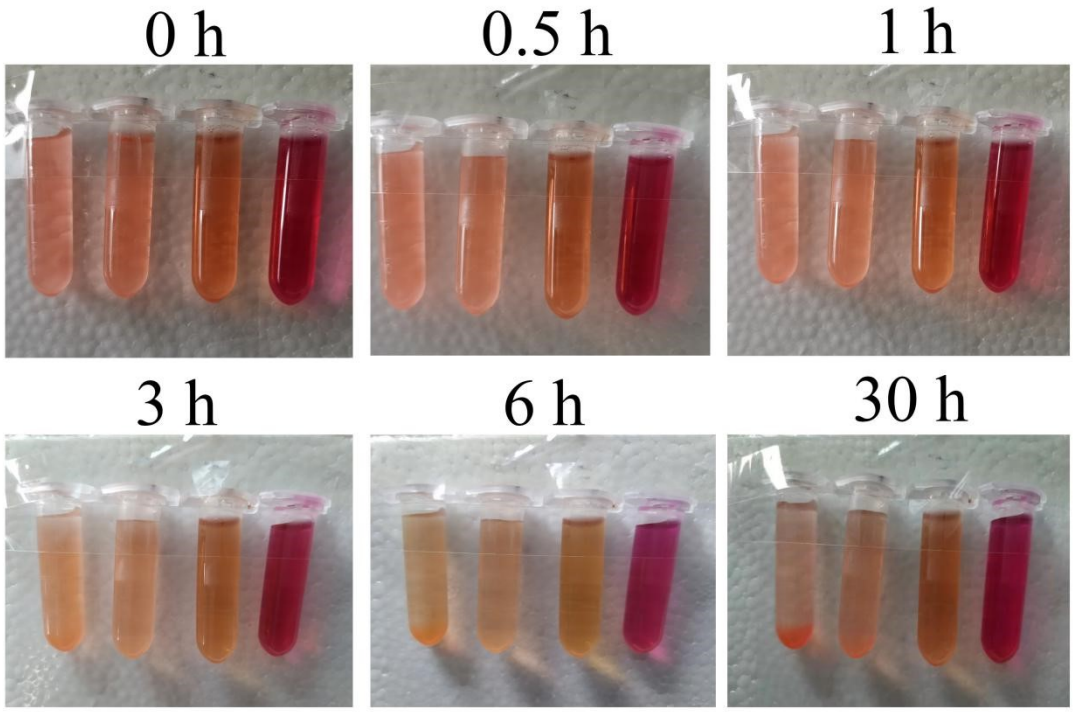

Figure S4. The biostability photographs of DOX/2DG@RENPs.

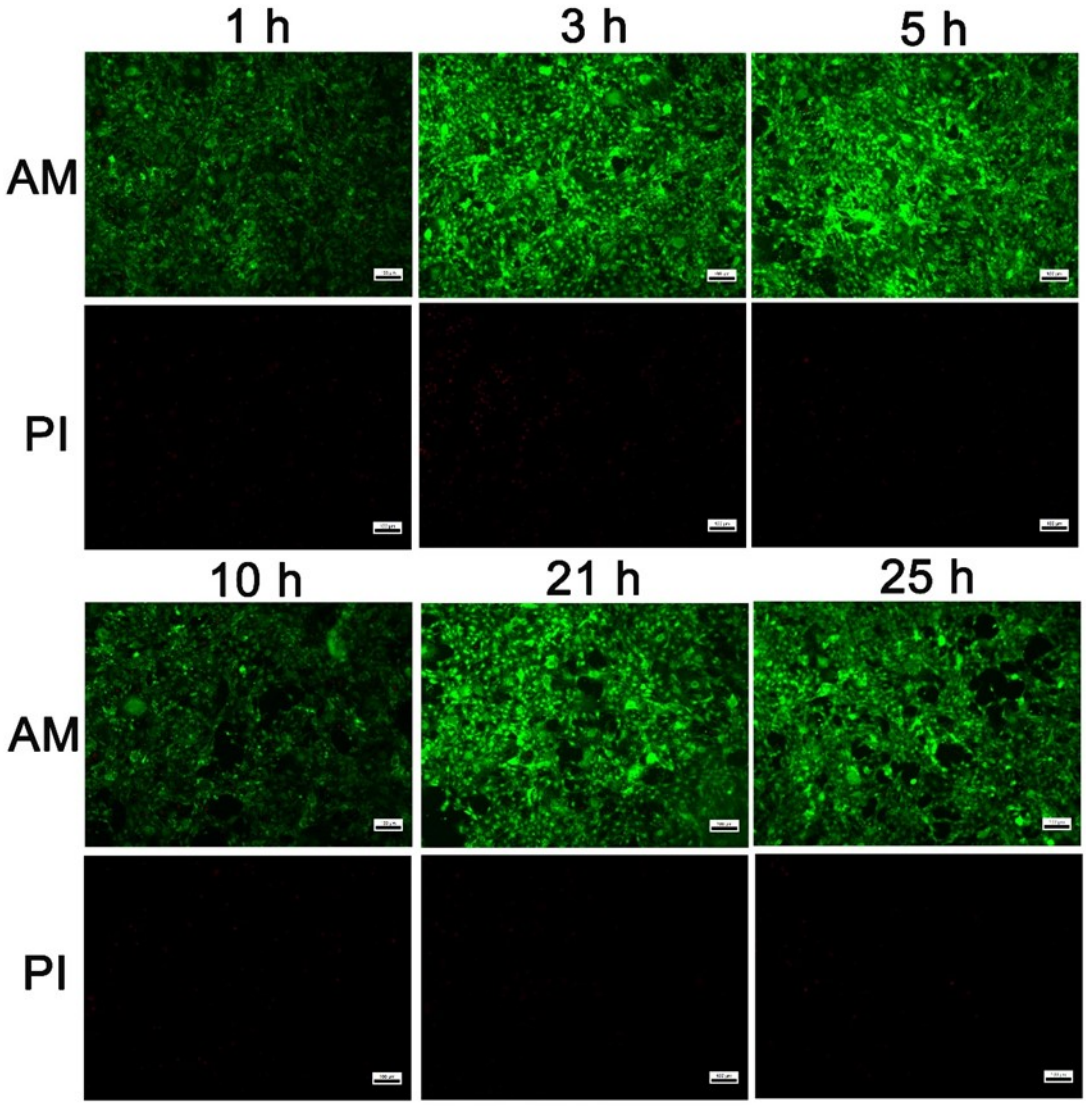

Figure S5. The fluorescence imaging of RENPs was detected by AM/PI for dead and living cells.

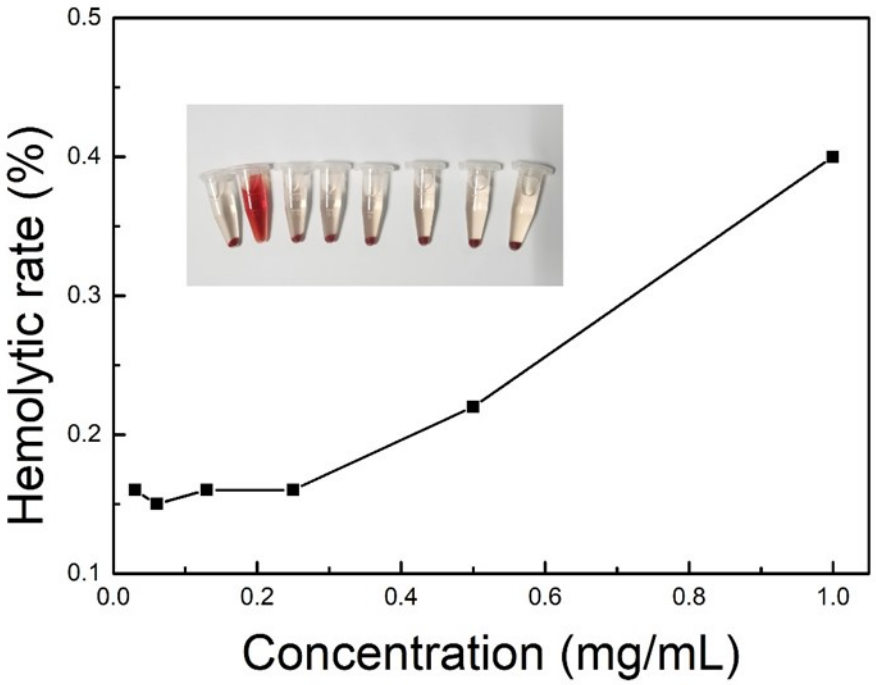

Figure S6. The hemolysis rate of the RENPs.

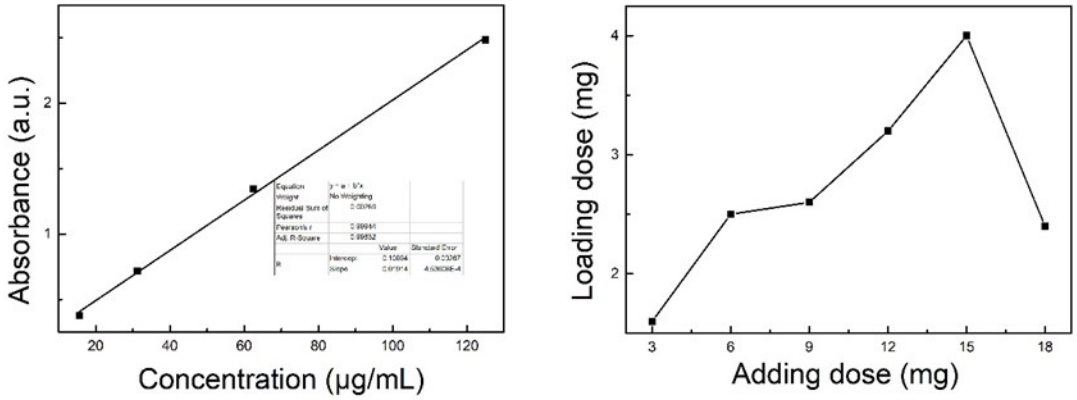

Figure S7. The graph of DOX was added with different weights

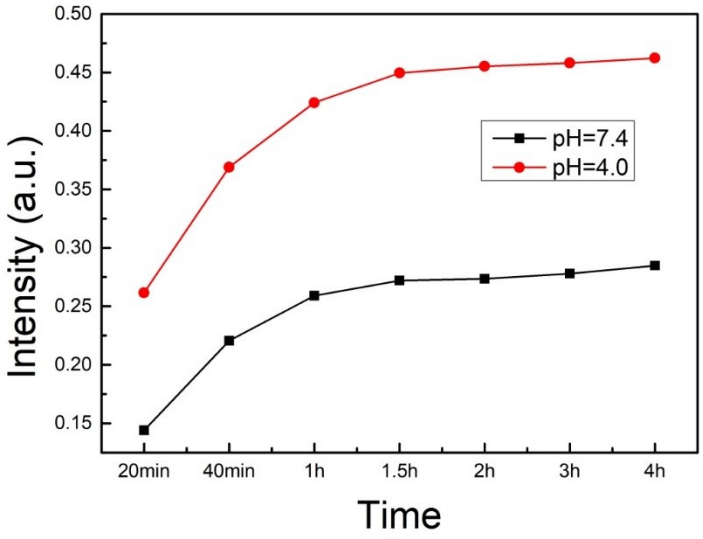

Figure S8. The DOX release rate curves of 2DG/DOX@RENPs.

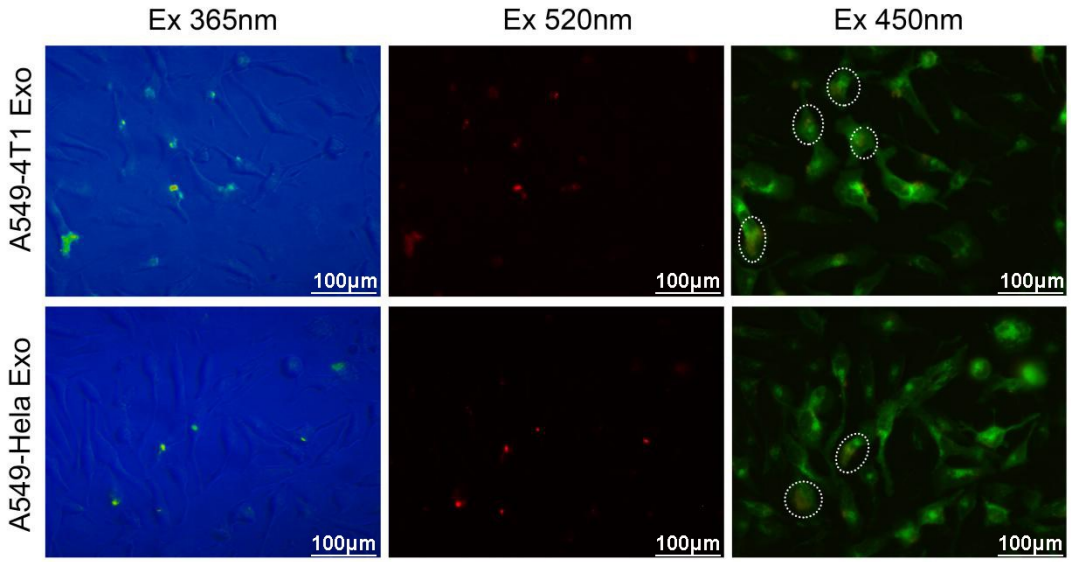

Figure S9. Fluorescence microscopy images of A549 cells co-incubated with E-RENPs of 4T1 cells or Hela cells, respectively.

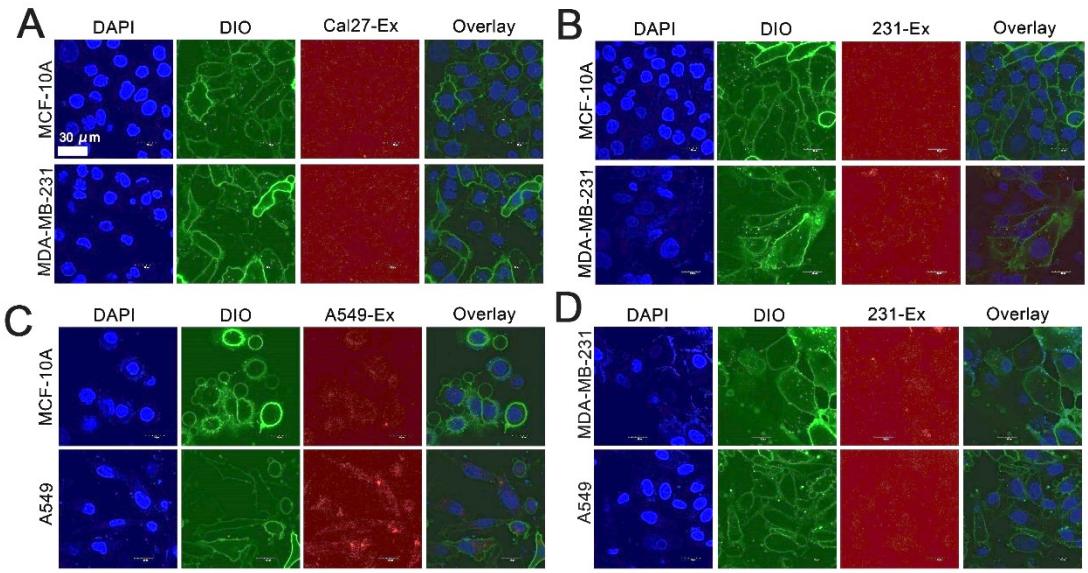

Figure S10. CLSM images of exosomes from different cell sources co-incubated with different cells. (A) Cal 27-Ex and (B) MDA-MB-231-Ex co-incubated with different cells of MDA-MB-231 and MCF-10A cells. (C) The A549-Ex co-incubated with different cells of A549 and MCF-10A cells. (D) The 231-Ex co-incubated with different cells of A549 and MDA-MB-231 cells.

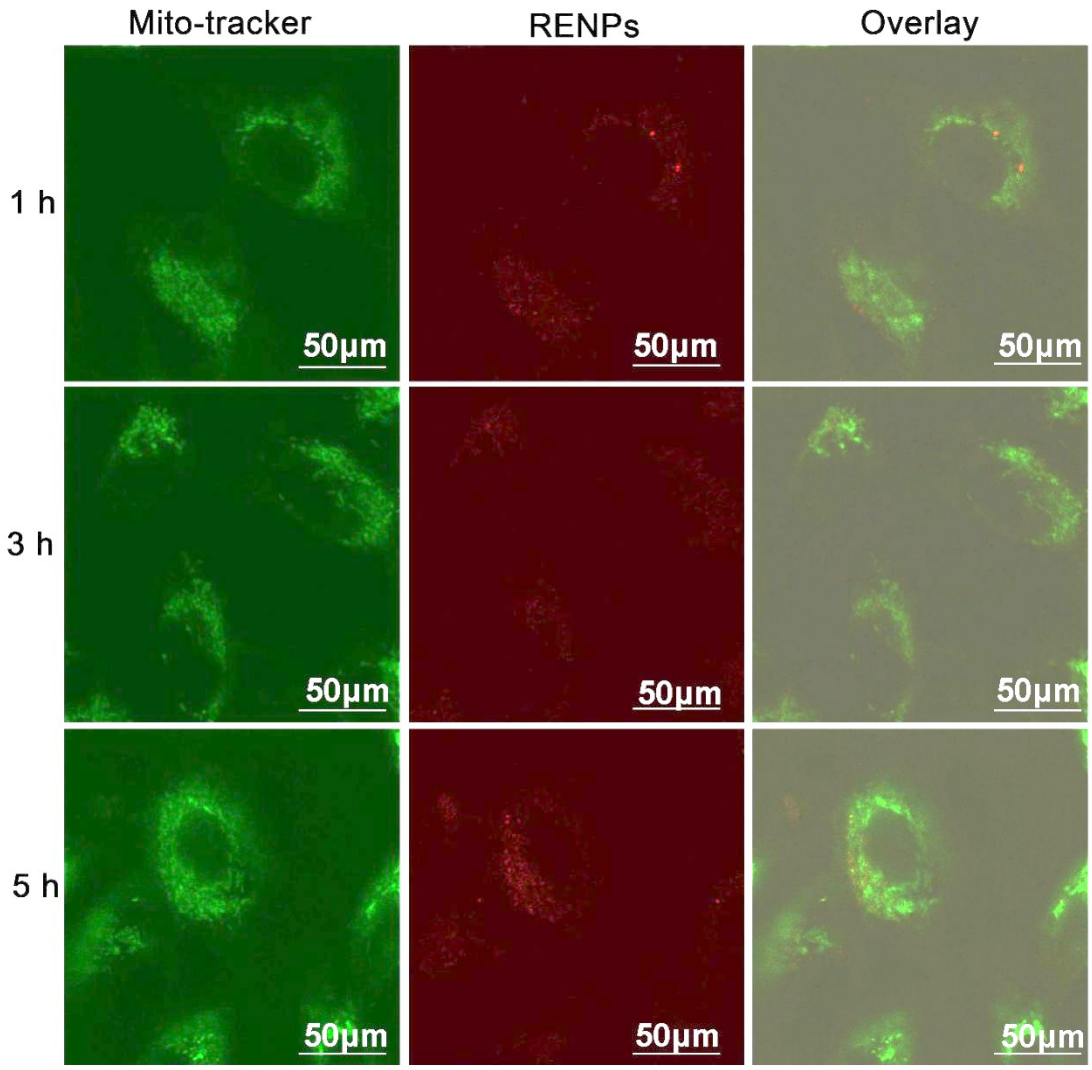

Figure S11. CLSM images of A549 cells incubated with RENPs at different time points.

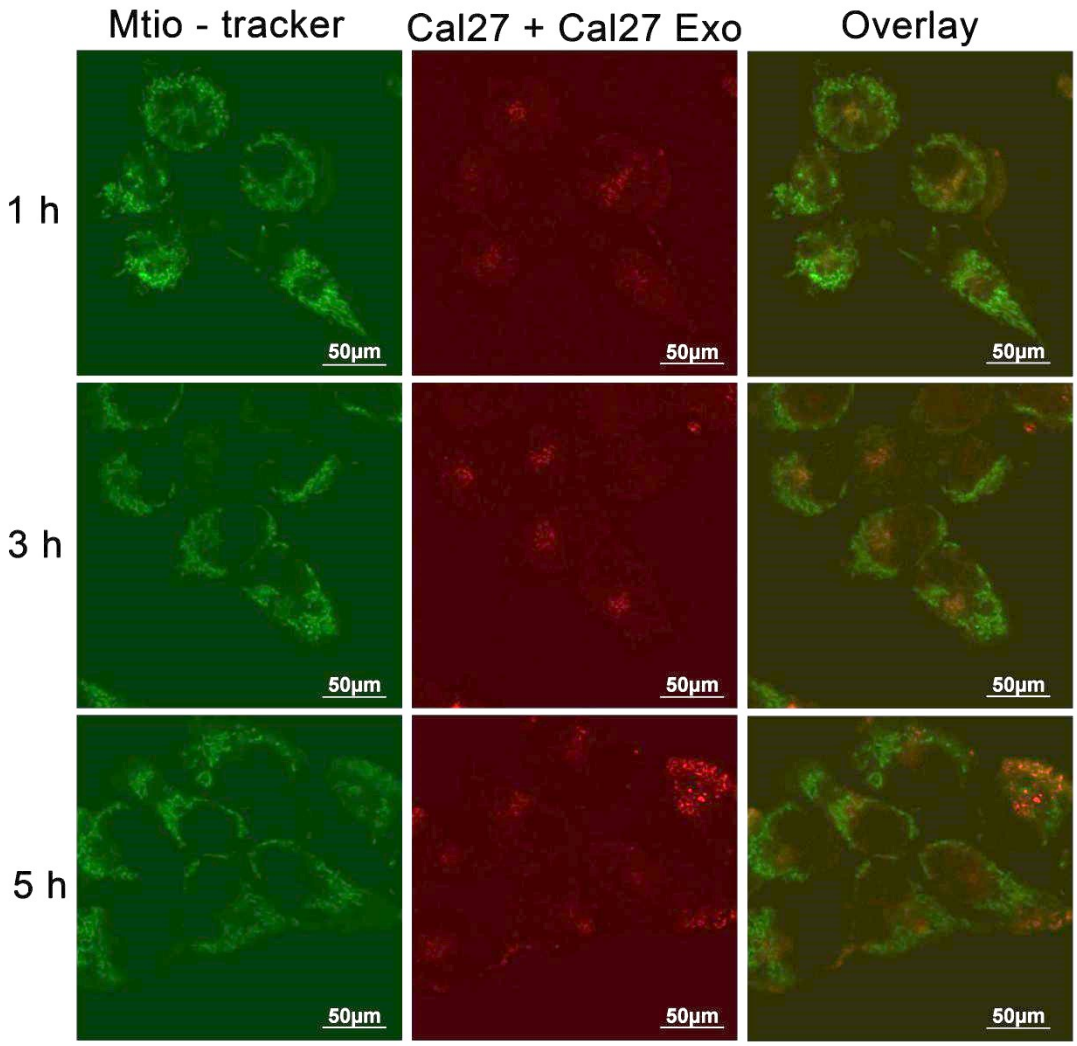

Figure S12. CLSM images of Cal27 cells incubated with E-RENPs from Cal27 cells at different time points.

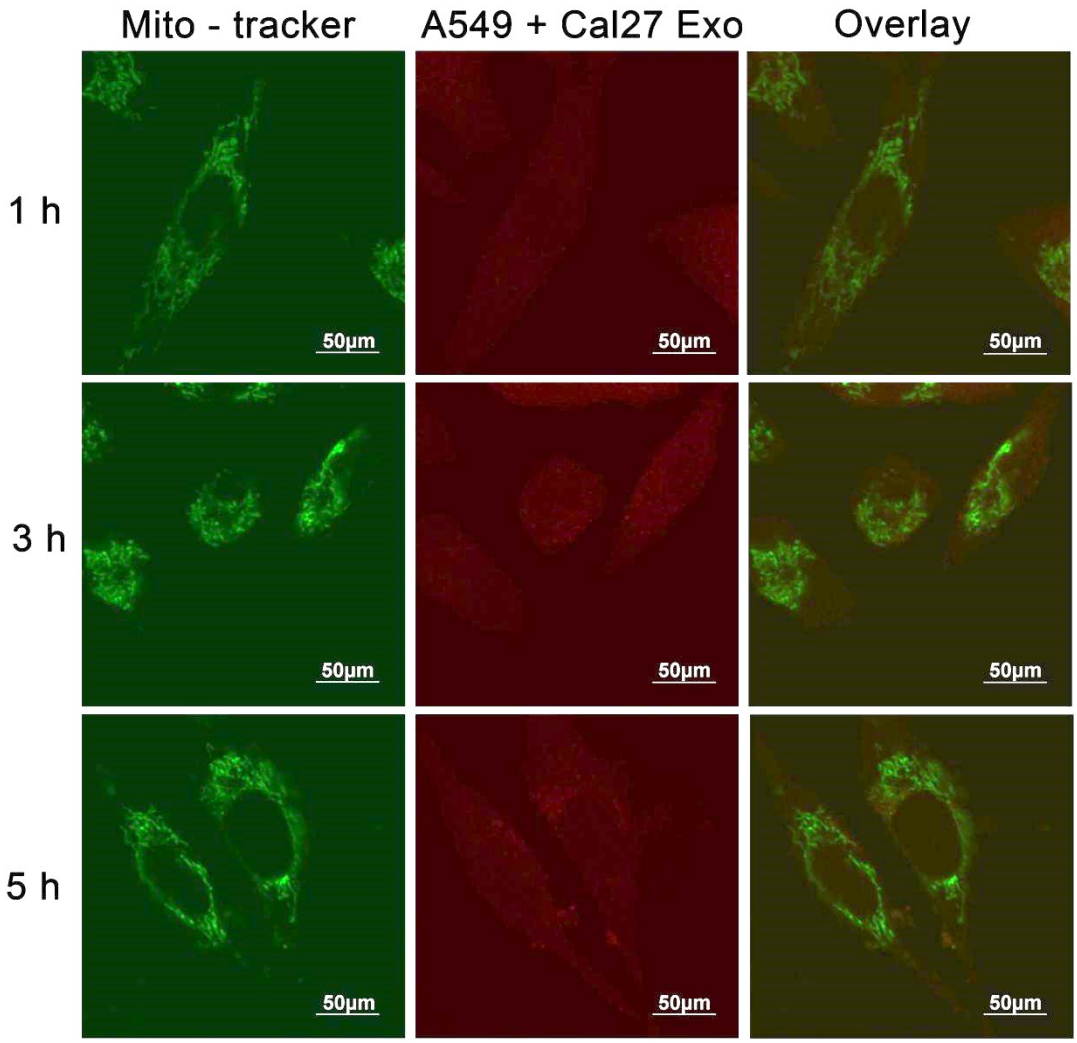

Figure S13. CLSM images of A549 cells incubated with E-RENPs from Cal27 cells at different time points.

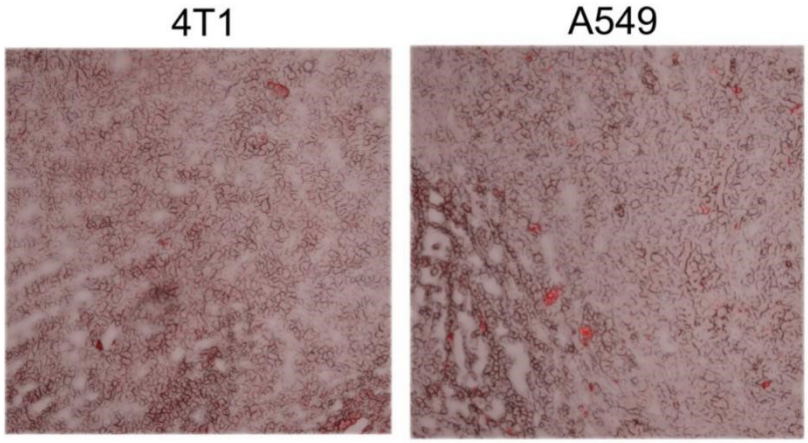

Figure S14. The pathological sections of 4T1 and A549 tumor.

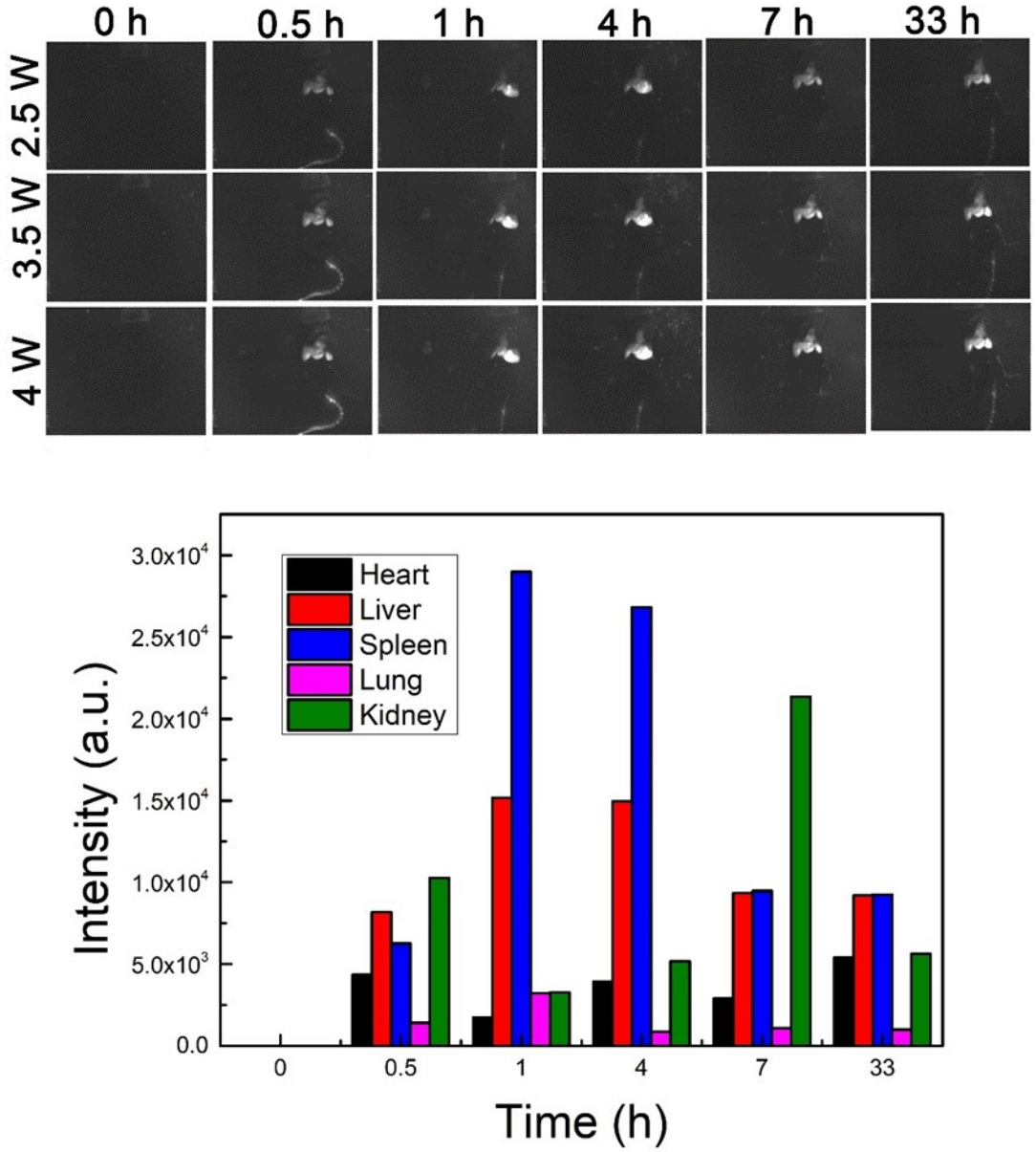

Figure S15. *In vivo* biodistribution photograph of the mice and the quantitative analysis of RENPs detected by the NIR II imaging under 980 nm excitation.

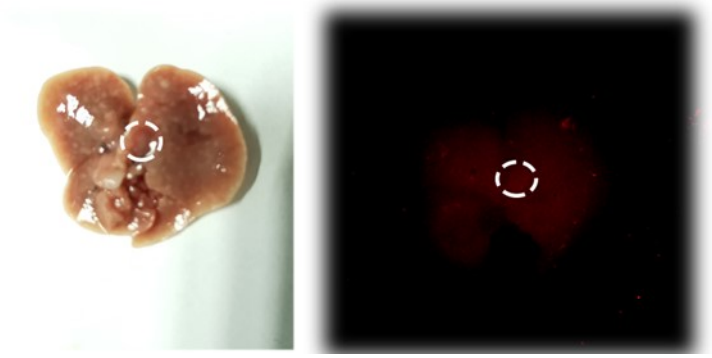

Figure S16. The fluorescence imaging photograph of liver metastases are sprayed of the E-RENPs.

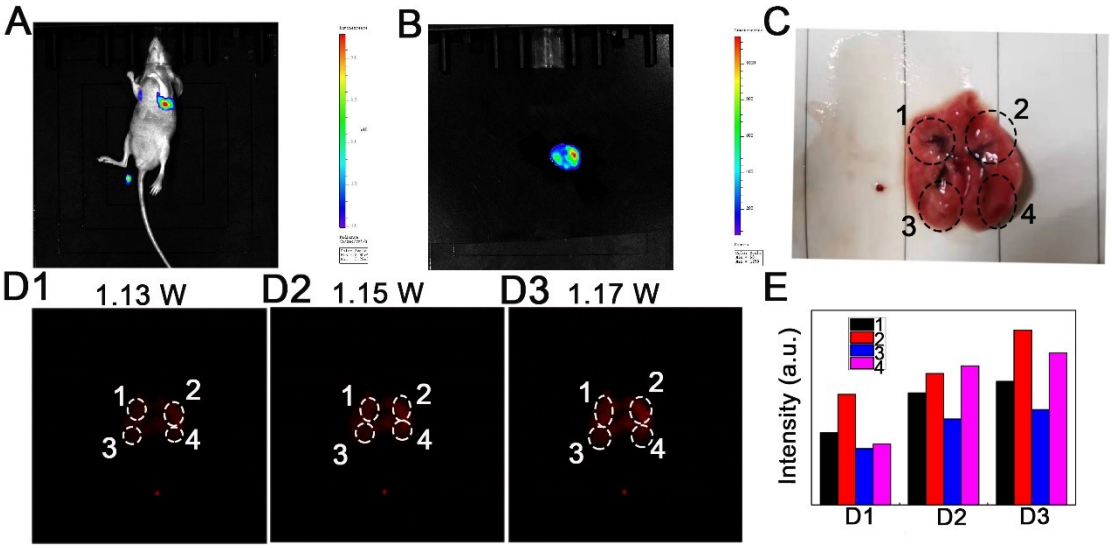

Figure S17. The lung of mice was dissected and recorded from another side. The Luc-fluorescence imaging of (A) the mice and (B) with lung dissected. (C) The photograph of in vitro lung metastasis. (D1-D3) The NIR II imaging image of the dissected lung tissue marked by E-RENPs and (E) their corresponding semi-quantitative analysis.

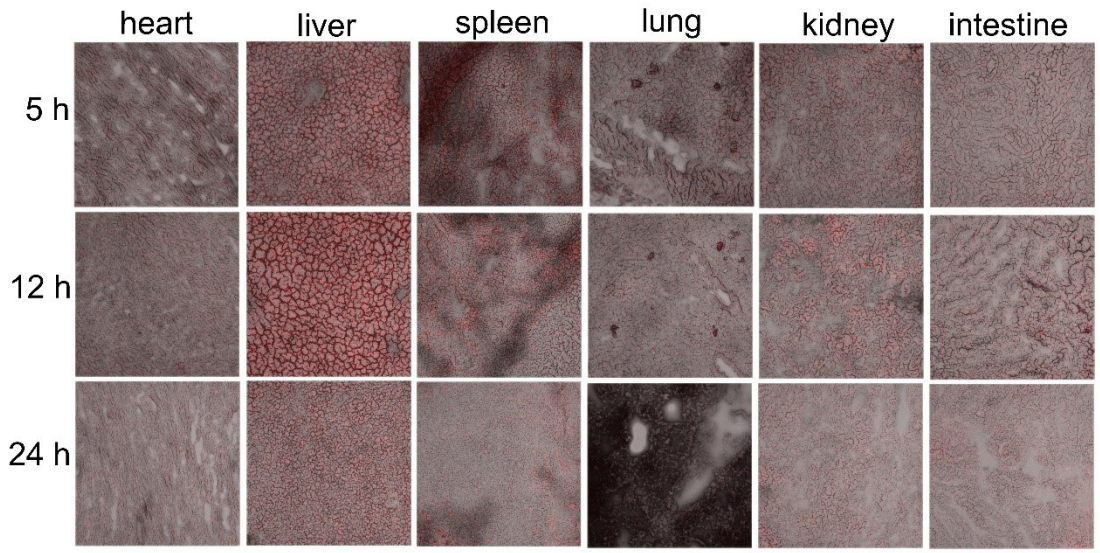

Figure S18. Fluorescence image of biological distribution in heart, liver, spleen, lung, kidney and intestine sections at different time points (5-24 h).

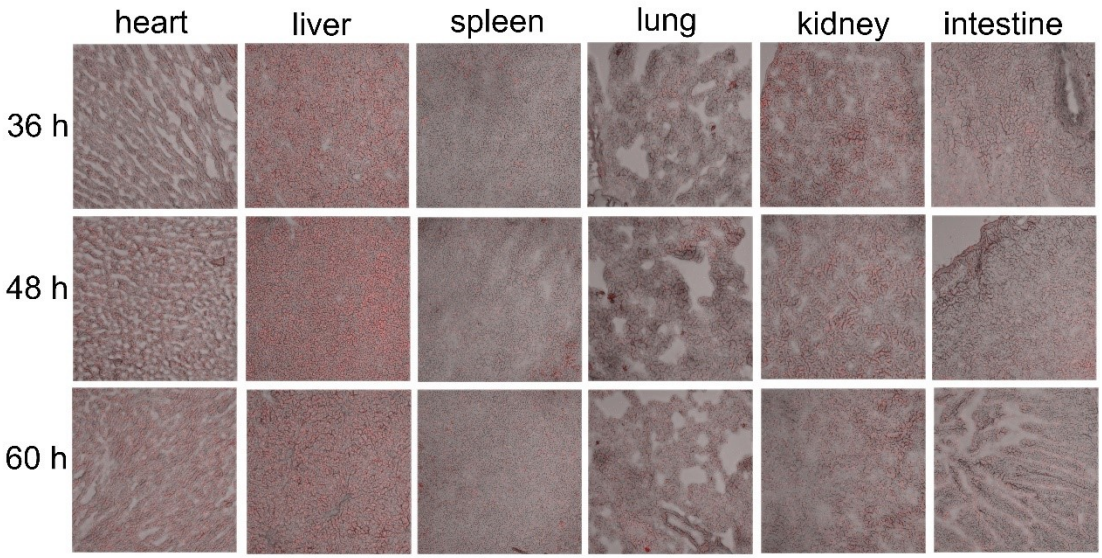

Figure S19. Fluorescence image of biological distribution in heart, liver, spleen, lung, kidney and intestine sections at different time points (36-60 h).

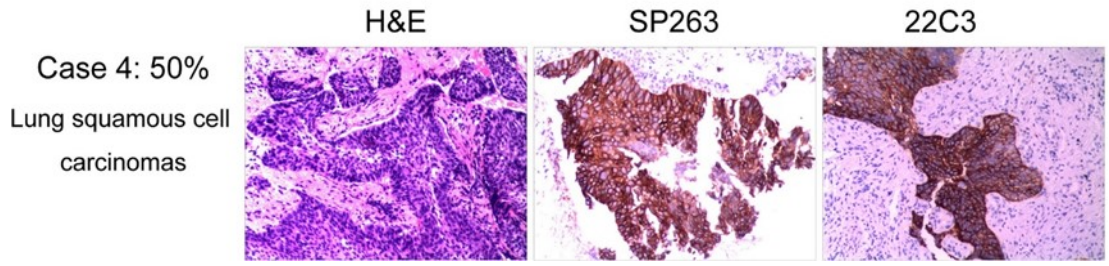

Figure S20. Pathology and immunohistochemistry microscopy images (using SP263 and 22C3 to mark PD-L1, respectively) of typical patients with lung adenocarcinoma.